

**NANO EXPRESS**

**Open Access**



# Effect of Ag Templates on the Formation of Au-Ag Hollow/Core-Shell Nanostructures

Chi-Hang Tsai<sup>1</sup>, Shih-Yun Chen<sup>2</sup>, Jenn-Ming Song<sup>3\*</sup>, Mitsutaka Haruta<sup>4</sup> and Hiroki Kurata<sup>4</sup>

## Abstract

Au-Ag alloy nanostructures with various shapes were synthesized using a successive reduction method in this study. By means of galvanic replacement, twined Ag nanoparticles (NPs) and single-crystalline Ag nanowires (NWs) were adopted as templates, respectively, and alloyed with the same amount of  $\text{Au}^+$  ions. High angle annular dark field-scanning TEM (HAADF-STEM) images observed from different rotation angles confirm that Ag NPs turned into AuAg alloy rings with an Au/Ag ratio of 1. The shifts of surface plasmon resonance and chemical composition reveal the evolution of the alloy ring formation. On the other hand, single-crystalline Ag NWs became Ag@AuAg core-shell wires instead of hollow nanostructure through a process of galvanic replacement. It is proposed that in addition to the ratio of Ag templates and Au ion additives, the twin boundaries of the Ag templates were the dominating factor causing hollow alloy nanostructures.

**Keywords:** Galvanic replacement, AuAg alloy rings, Ag@AuAg core-shell wires

## Background

AuAg alloy nanostructures with zero or one dimension (0-D or 1-D) exhibit unique optical and catalytic properties and have diverse applications, e.g., catalytic converters and electrode catalysts for Li batteries [1–8]. Alloying of Au and Ag gives rise to the combination of performance between the metal components and has a variety of applications, including tunable localized surface plasmon resonance features [9], surface enhanced Raman scattering [10–12], optical imaging [13–15], photothermal therapy [16], and encapsulation [17]. As for the catalytic properties, previous reports show that AuAg alloy nanoparticles (NPs) exhibit superior catalytic activity for CO oxidation compared with pure Au and Ag NPs, also due to the synergistic effect [7, 8, 18].

The synthesis and the formation of alloy nanostructures have attracted considerable attention. The most common way to prepare AuAg nanostructures is through the chemical reduction method [19, 20]. AuAg NPs can be reduced from the solution with a mixture of Au and Ag ions containing precursors. In these cases, Ag NPs are usually used as the templates, and Au ions are added for

alloying [19]. To synthesize AuAg alloy NPs, another method proposed by Crespo et al. is the mild decomposition of the single-source organometallic precursor [21]. In this case, the composition, size, as well as the surface plasmon resonance of AuAg NPs, can be easily controlled by adding different amounts of hexadecylamine (HDA). Crespo et al. [22] also suggested an organometallic approach by using HDA-capped Ag as templates. By controlling the concentration of  $[\text{Au}(\text{C}_6\text{F}_5)(\text{tht})]$  ( $\text{tht}$  = tetrahydrothiophene), Ag@Au nanostructures with different shapes can be prepared, including circles, hexagons, triangles, truncated triangles [22].

Table 1 lists some relevant studies on the synthesis of AuAg nanostructures. These nanostructures can be categorized into two groups, viz., solid structure and hollow structure. It has been suggested that by adjusting the ratio of Ag templates and Au ion additives, Ag@Au or Ag@AuAg core-shell nanostructures can be obtained [19, 22, 23]. The concentration of the Au precursors plays an important role in the replacement reaction of Ag by Au, and the structure, morphology, as well as the composition, can thus be controlled. The excessive galvanic reaction between Au and Ag might give rise to the formation of hollow structures [6, 24–30], e.g., AuAg hollow particles and tubes. As also tabulated in Table 1, the characteristics of Ag templates, e.g., the existence of

\* Correspondence: samsong@nchu.edu.tw

<sup>3</sup>Department of Materials Science and Engineering, National Chung Hsing University, Taichung 402, Taiwan

Full list of author information is available at the end of the article

**Table 1** A summary of prior works of Au-Ag alloy nanostructures

Structures	Ag template crystal	Ag template size	Ag specific surface area ( $\text{nm}^{-1}$ )	AuAg nanostructure size (nm)	Ref.
Solid	AuAg NPs	n/a	6.1 nm	0.98	13
	AuAg NPs	n/a	7.4 nm	0.81	16
	Ag@Au NPs	n/a	9.6 nm	0.63	15
	AuAg NPs	n/a	20.7 nm	0.29	~20
	Ag@Au NPs	n/a	9.8 nm	0.61	$\text{Ag}_{\text{core}} = 8.1, \text{Au}_{\text{shell}} = 6$
	Ag@AuAg NPs	Single crystalline	18.6 nm	0.32	n/a
	Ag@AuAg NWs	Single crystalline	$d = 90 \text{ nm } h = 10 \mu\text{m}$	0.02	$\text{Ag}_{\text{core}} = 85, \text{AuAg}_{\text{shell}} = 6$
Hollow	AuAg hollow NPs	Twinned	11 nm, 14 nm	0.42, 0.54	$d_{\text{inner}} = 12.4, d_{\text{outer}} = 16.9$
	AuAg hollow NPs	n/a	41 nm	0.14	46–53
	AuAg hollow NPs	Twinned	53 nm	0.11	68
	AuAg hollow NPs	n/a	20–100 nm	0.3–0.06	$d_{\text{inner}} = 88, d_{\text{outer}} = 128$
	AuAg hollow NPs	Twinned	75 nm	0.08	n/a
	AuAg nanotubes	Twinned	$d = 50 \text{ nm}$	n/a	n/a
	AuAg nanotubes	Twinned	$d = 30–60 \text{ nm } h = 1–50 \mu\text{m}$	0.06–0.13	n/a
	AuAg nanorings	Twinned	14 nm	0.42	$d_{\text{inner}} = 2–4.5, d_{\text{outer}} = 12–15$

n/a means not available

planar defects (twins in this case), size, and specific surface area of templates, may also affect the morphology of the AuAg nanostructures. However, there is still a lack of studies regarding Ag templates.

In order to clarify the dominant factors determining the formation of hollow AuAg alloy nanostructures, two kinds of templates, with a variety of differences, twinned Ag NPs and single-crystalline Ag nanowires (NWs), were used. The same moles of Au ions were added for alloying. In combination with the cases given in Table 1, the effect of the Ag templates will be investigated. In addition, to study the hollow structure in depth, the HAADF images of the nanostructures from different angles will be observed.

## Methods

### Preparation of Au-Ag Nanostructures

The processes for preparing Au-Ag nanostructures with different dimensions are illustrated in Fig. 1.  $\text{AgNO}_3$  and  $\text{HAuCl}_4$  aqueous solutions with the same concentrations (0.4 mM) are the precursors. Figure 1a shows the procedures for the synthesis of 0-D Au-Ag structures. The templates, Ag NPs, were obtained from the reduction of  $\text{AgNO}_3$  using a mixed solution with 1 wt% of  $\text{NaBH}_4$  and 1 wt% of  $\text{Na}_3\text{C}_6\text{H}_5\text{O}_7$ . 0.29 mM (MW 55,000 g/mol) PVP, the surfactant to prevent particle aggregation, was dissolved in water by stirring for 6 min at 95 °C. As indicated in Fig. 2a, b, the Ag NPs thus produced are heavily twinned with an average particle size of 14 nm. The interplanar distance of 0.23 nm can be referred to {111} planes of Ag.  $\text{HAuCl}_4$  aqueous solution was then mixed with the Ag NP suspensions and agitated at 95 °C for 15 min.

With respect to 1-D nanostructures, single-crystalline Ag NWs were prepared via thermally-assisted photoreduction; the procedures of which have been described in previous works [31]. Fifteen-microliter droplets of 0.1 M  $\text{AgNO}_3$  aqueous solution were dropped on the annealed  $\text{TiO}_2$  substrates, followed by a post-heat treatment in an IR furnace. The samples were heated isothermally at 300 °C for 3 h and then furnace-cooled. The diffraction pattern inserted in Fig. 2c demonstrates that the Ag NWs thus synthesized are single crystalline with the  $[1\bar{1}0]$  growth direction. The average wire length and diameter are 10 μm and 90 nm, respectively. In order to form 1-D AuAg nanostructure,  $\text{HAuCl}_4$  aqueous solution was mixed with the Ag NW suspensions and agitated at 200 °C for 3 hr.

### Microstructural and Characteristic Analyses

The UV-visible spectra of the nanostructures solutions were measured by a spectrophotometer (Varian Cary 100 UV-Visible spectrometer) with a 10 mm quartz cell. The electron microscope used in this study was a TEM/STEM (TEM, JEM-2200FS, JEOL, Japan) operated at 200 kV, equipped with an energy dispersive X-ray spectroscopy (EDS). High angle annular dark field-scanning TEM (HAADF-STEM) images were collected over scattering angles from –30 to 30 mrad ( $X$  and  $Y$  axes).

## Results and Discussion

Figure 3 illustrates the UV-visible absorption spectra of the templates and the Au-Ag nanostructured thus obtained. The absorption peaks centered at 407 nm

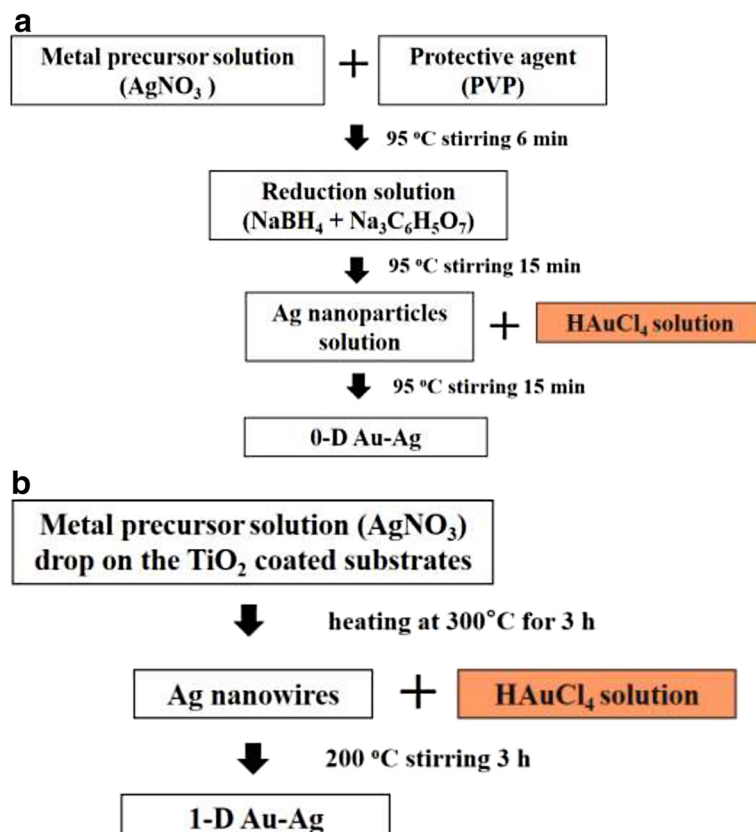
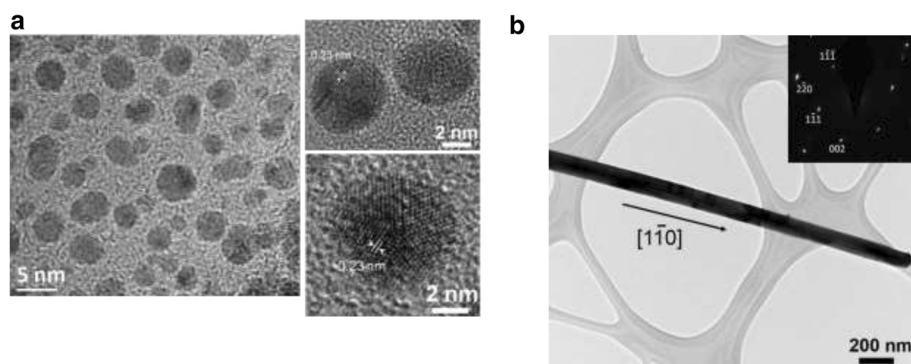


**Fig. 1** Synthetic process of **a** Au-Ag zero-dimensional structure and **b** Au-Ag one-dimensional structure

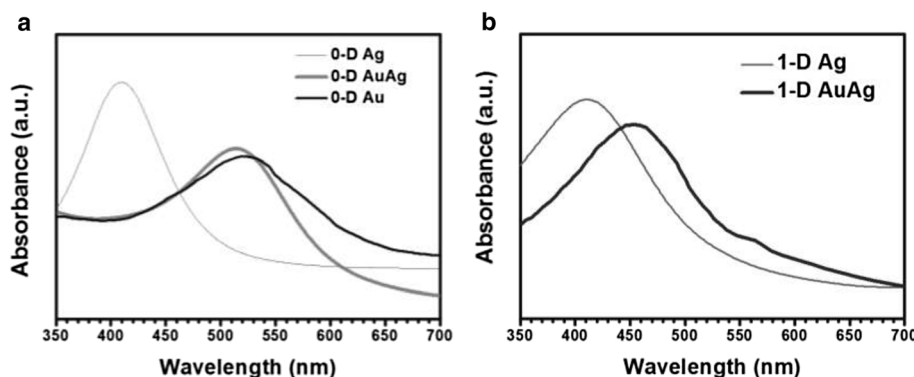
for Ag NPs and 408 nm for Ag NWs, respectively, due to surface plasmon resonance, are identical to the reported value [25, 32–33]. After being reacted with HAuCl<sub>4</sub> solution, a small red shift for the absorption peaks could be observed. As illustrated, the absorption peak was 506 nm for 0-D nanostructures, while that for 1-D nanostructures was 455 nm, and both the wavelengths were lower than Au NPs in the

literature [34, 35]. The fact that the optical absorption spectrum shows only one plasmon band reveals that the surface of the 0-D and 1-D Au-Ag nanostructures was alloy rather than individual Au and Ag.

Electron microscopic observation (Fig. 4) indicates that the 0-D nanostructures are hollow and exhibit an average size of  $20 \pm 3.5$  nm, as well as an identical interplanar distance with Ag NPs (Fig. 4b). The HAADF



**Fig. 2** TEM images of templates **a** Ag NPs of zero-dimensional structure: (right) twined Ag NPs and (left) magnified images showing lattice fringes and **b** Ag NWs of one-dimensional structure and the inserted diffraction pattern



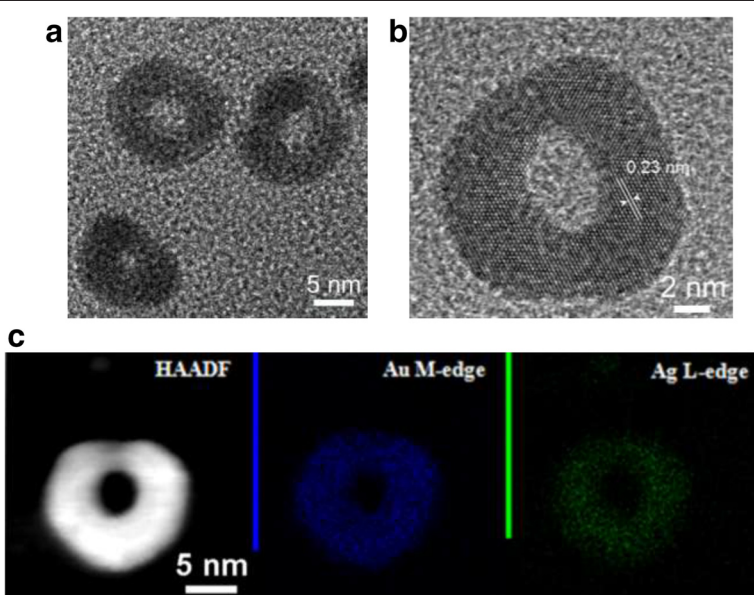
**Fig. 3** UV-vis absorption spectra: **a** zero-dimensional structure and **b** one-dimensional structure

image and EDS elemental mapping further verify that the nanostructures are composed of Au and Ag in the form of uniform alloy (Fig. 4c). EDS quantitative results show the Ag content of the hollow structures was about 51 at. % (Table 2). A recent report studied hollow AuAg alloy rings and the composition effect on the segregation of Au and Ag based on the EDS elemental mapping data [36]. However, our observation found no such segregation.

Moreover, high-resolution TEM (HRTEM) images taken from the near-edge regions of the 1-D Au-Ag nanostructures and corresponding selected area diffraction patterns (SADPs) given in Fig. 5a reveal that the core-shell feature of the 1-D nanostructures, of which the core was single-crystalline Ag wires, and the shell deposits, compact and attached firmly to the Ag surface, with thickness of  $4 \pm 0.3$  nm comprised nanocrystals showing an interplanar

distance of 0.23 nm. Similar to the hollow structure in Fig. 4, the HAADF image of the 1-D nanostructure as well as EDS elemental mapping further suggest the nanostructures are alloy of Au and Ag possessing Ag content of 56.2 at. % (Table 2). That the Ag signal at the edge region is less bright than Au further confirms the core-shell structural feature of the galvanic-reacted NWs. The above results may reveal that in the absence of surfactants and grain boundaries, a clean surface of single-crystalline Ag NWs is conducive to the precipitation of AuAg alloys.

The literature claims that the 0-D Au-Ag nanostructure formed through galvanic replacement between Ag atom and Au ions are mostly core-shell NPs or hollow spheres [6, 19, 22–30]. In order to clarify this issue, the 0-D hollow structures synthesized in this study were examined by HAADF-STEM images from different



**Fig. 4** Microstructural observation results of the 0-D Au-Ag nanostructures: **a** TEM image and **b** HRTEM image and **c** HAADF image and EDS elemental mapping

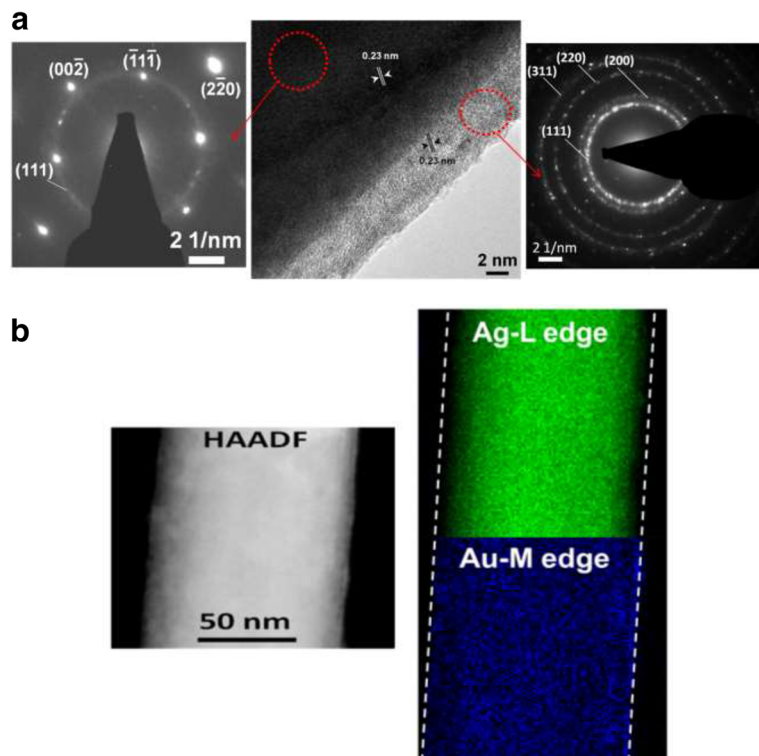


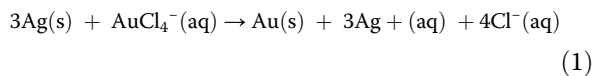
**Fig. 5** Microstructural observation results of the 1-D Au-Ag nanostructures: **a** HRTEM images and selected area diffraction patterns (SADP) and **b** HAADF image and EDS elemental mapping of Ag (upper) and Au (lower)

angles (Fig. 6). Observations from continuous rotation along  $X$  and  $Y$  axes ranging from  $-30^\circ$  to  $30^\circ$ , verify that the hollow structures were rings rather than hollow spheres or core-shell particles. It can be speculated that previous studies might have misjudged the morphologies. For instance, the rings in the photos 30 rotated along the  $X$ -axis and  $-30^\circ$  along the  $Y$ -axis resemble hollow or core-shell particles. In addition, a quantitative data estimating the inner and outer diameters of the alloy nanorings were obtained through TEM image analysis. Figure 7 indicates that the outer diameter of the nanorings ranged from  $12\sim15$  nm, while the inner diameter was between  $2\sim4.5$  nm.

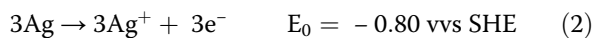
By means of terminating the alloying process, the UV-vis absorption peaks of the 0-D nanostructure subjected to different periods of galvanic replacement reaction are illustrated in Fig. 8a. Figure 8b shows the wavelength of those absorption bands of the 0-D nanostructures and the corresponding Au content

measured by EDS. It is surprising that at the first 10 s, the absorption peak located at 559 nm reveals the signal was from Au-rich nanostructures instead of Ag. The chemical composition data at 30 s showing  $\sim 82$  at. % Au verifies this observation. With an increase in reaction time up to 3 min, the absorption red shifted rapidly to 523 nm, and the Au content decreased to about 40 at. % as well. After that, the absorption band continued to move toward the long wavelength side, but slowly. The Au content rose to 50 at. % and then remained constant.

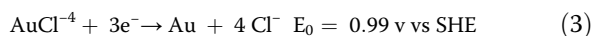
In the present study, the redox reaction along with those for the anodic dissolution and cathodic reduction are given as follows [37]:



Dissolution of Ag:



Reduction of Au ions:



SHE: standard hydrogen electrode

**Table 2** EDS results of AuAg nanorings and the shell of Ag@AuAg NWs (at. %)

Element (at. %)	0-D AuAg	Shell of 1-D AuAg
Ag	51.03	56.18
Au	48.97	43.82

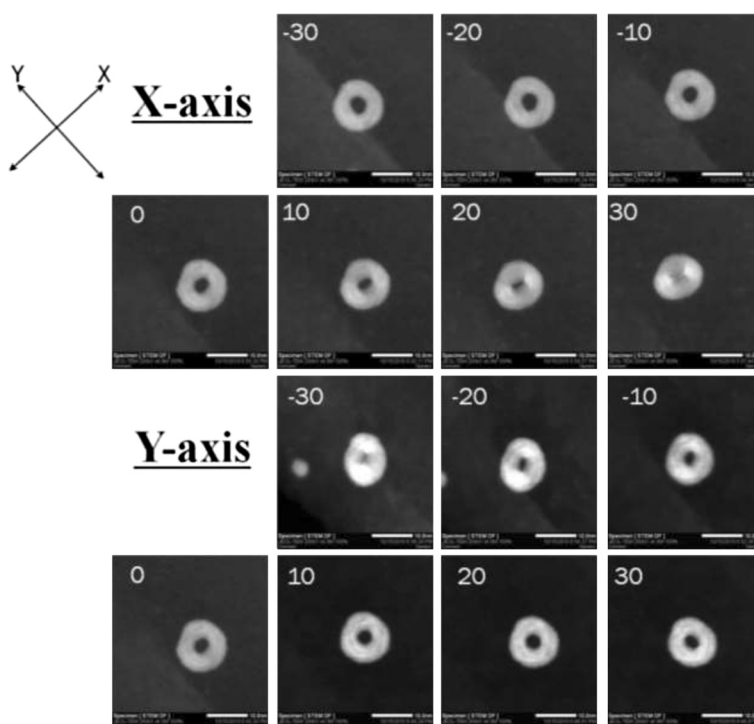


**Fig. 6** HAADF images of Au-Ag hollow particles with different rotation angles under STEM mode

The positive potential of the redox reaction gives rise to a spontaneous replacement of Ag by Au. However, due to the atomic valence, one Au atom replaces three Ag atoms [38], thus in the case of 0-D nanostructure, the Ag templates were consumed three times faster than the reduction and subsequent deposition of Au from the  $\text{HAuCl}_4$  solution. Therefore, as sketched in the upper diagrams in Fig. 9, Au ions obtained electrons from Ag atoms and thus rapidly dissociation of Ag NPs probably through the planar defects, i.e., twin boundaries in this

case. The complete consumption of Ag along with the precipitation of Au atoms formed Au ring-like nanostructures. The subsequent co-precipitation of Au and Ag with the assistance of residual reducing agents,  $\text{NaBH}_4$  and  $\text{Na}_3\text{C}_6\text{H}_5\text{O}_7$ , as well as the interdiffusion of Au and Ag, gave rise to the formation and growth of alloy rings with an approximate Au/Ag ratio of 1. It has been demonstrated experimentally and by theoretical calculations that the surface plasmon resonance (SPR) of hollow Au NPs red-shifts significantly relative to the SPR of solid Au NPs of the same size [39]. In this study, the observation of absorption maximum for 0-D nanostructures at wavelengths value (506 nm) being red-shifted compared to that of  $\text{Ag@AgAu}$  core-shell solid structure [23] indicates that the 0-D nanostructures here may be hollow. The slow blue shift after 3 min of reaction might have resulted from the thickening and coarsening of the ring structure, gradually approaching solid AuAg NPs [25].

With respect to 1-D Au-Ag nanostructure, AuAg alloy nanocrystals were deposited on the surface of Ag wires as a compact layer of nanocrystals. We suggest that there may have been two interfaces, the inner surface of the nanocrystalline deposit between Ag and reduced Au (interface I in Fig. 10) and the other one, the outer surface between reduced Au and solution (interface II in Fig. 10). Dissociation of Ag (Eq. 2) can be considered to have occurred at interface I, while the reduction of Au

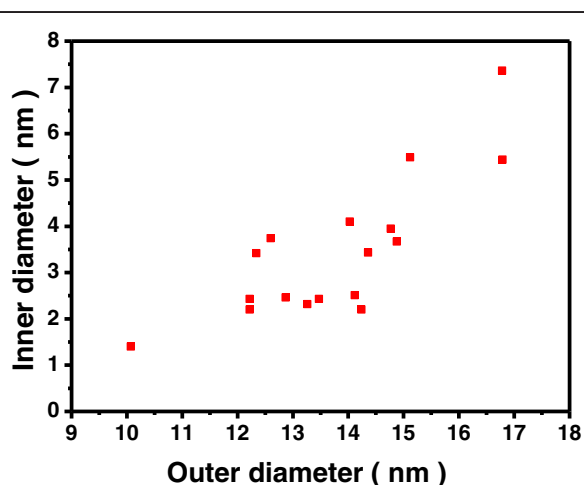


**Fig. 7** Outer diameters and inner diameters of the Au-Ag nanorings

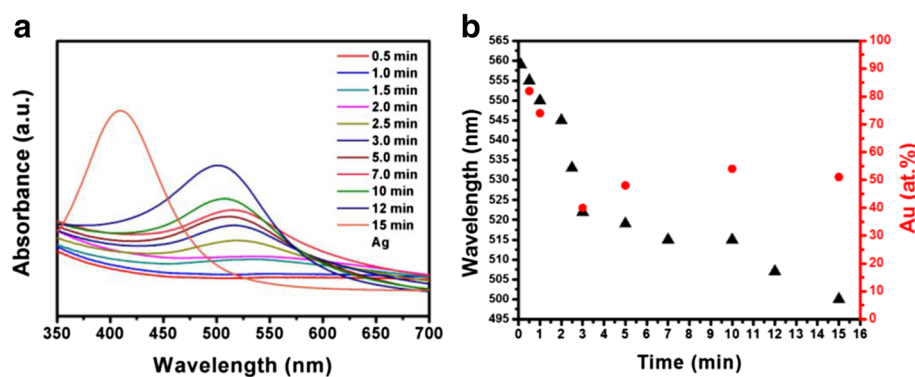


**Fig. 8** (a) UV-vis spectra and (b) wavelength of absorption peaks and Au content as a function of galvanic reaction time in the case of AuAg nanorings

took place at interface II (Eq. 3). There is no evidence so far showing the orientation relationship between single-crystalline Ag and nanocrystalline deposits. However, it can be inferred that boundaries in between nanocrystals provided large quantities of microchannels for the transportation of Ag ions, and thus Ag ions generated at interface I could transfer rapidly through the Au deposit. On the other hand, the electrons could travel through highly conductive deposits easily to support the reduction of Au ions at interface II. Meanwhile, it can be deduced that not only the galvanic reaction but also the interdiffusion of Au and Ag proceeded to turn Au deposits into AuAg alloy shell. The chemical composition shown in Table 2 led us to believe that the Au/Ag ratio of 1 is the stablest composition for interdiffusion products. This may be due to the iso-morphous feature of this binary system (Au and Ag

are mutual soluble at any composition) and the minimum free energy caused by the high entropy of mixing [40].

With the same concentrations of metallic ions in the precursor solutions, the selection of Ag templates caused quite different nanostructures, i.e., AuAg alloy hollow structure, more precisely, nanorings when Ag NPs were adopted as templates, and Ag@AuAg core-shell NWs in the case of Ag NW templates. Such differences can be attributed to two factors, specific surface area as well as the planar defects. Compared with Ag NWs ( $0.02 \text{ nm}^{-1}$ ), a much greater specific surface area of Ag NPs ( $0.42 \text{ nm}^{-1}$ ) may result in an accelerated kinetics for galvanic replacement. However, in comparison with the previous studies listed in Table 1, it can be deduced that the planar defects (twin boundaries) within the Ag templates are the key achieving a

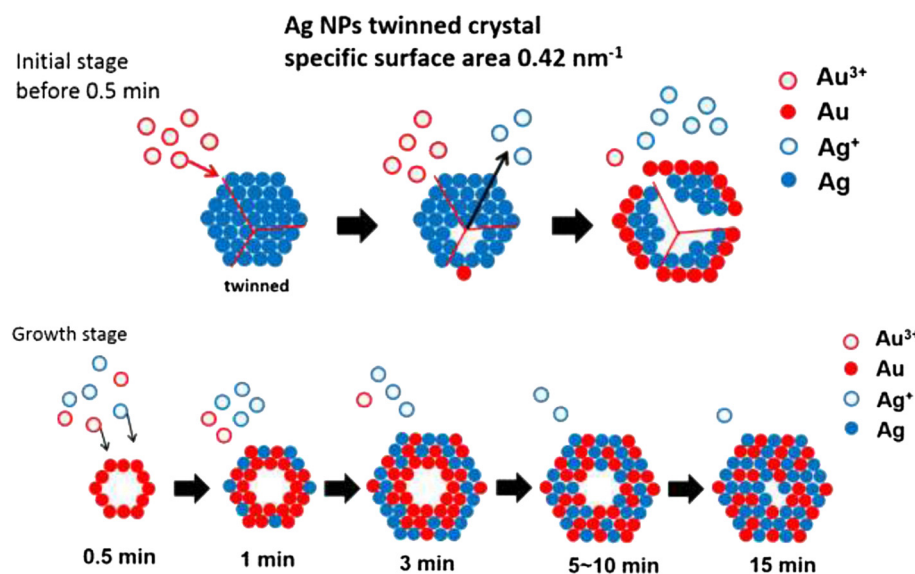
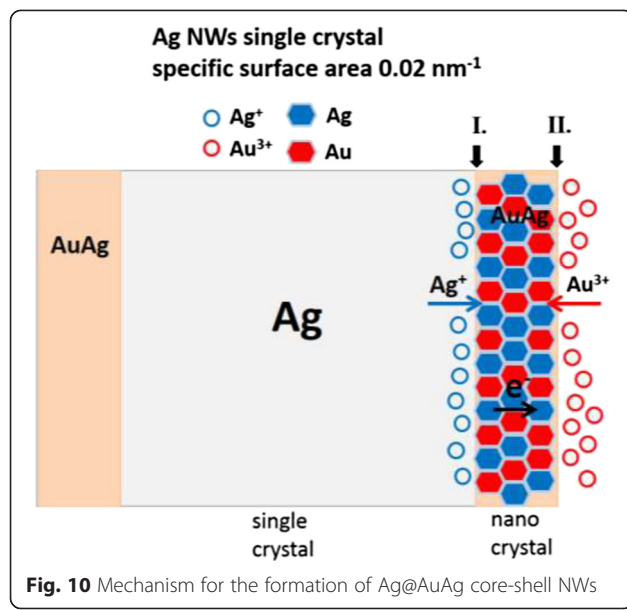


**Fig. 9** Mechanism for the formation of Au-Ag nanorings



hollow structure instead of the size, shape, and the specific surface area. Subjected to galvanic replacement with sufficient Au ions, single-crystalline NPs/NWs turn into AuAg sold structures, while those with twins form a hollow alloy structure. Along twin boundaries, which are regarded as the fast diffusion path, the Ag templates decomposing from inside and being consumed at the very early stage are a prerequisite to the formation of the unique ring structure.

## Conclusions

The morphology and shape of Au-Ag nanostructures can be tuned through the selection of Ag templates in galvanic replacement process. Reacted with Au ions, Ag NPs turned into AuAg alloy rings with the Au/Ag ratio of 1. The characteristics of the alloy ring structure, as well as details of its formation were documented. In contrast, single-crystalline Ag NWs became Ag@AuAg core-shell wires instead of a hollow nanostructure. Combined with the relevant literature, it can be suggested that twin boundaries supporting fast diffusion path for the decomposition of Ag templates are the dominating factors in the formation of hollow/ring alloy nanostructures.

## Competing Interests

The authors declare that they have no competing interests.

## Authors' Contributions

CHT carried out the main part of synthetic and analytical works, participated in the sequence alignment, and drafted the manuscript. SYC participated in the discussion of the growth mechanism. JMS participated in the design of the study, draft preparation, and coordination. MH and HK carried out the observation of STEM/HAADF images. All authors read and approved the final manuscript.

## References

- Liu S, Chen G, Prasad P N, Swihart M T, Synthesis of monodisperse Au, Ag, and Au-Ag Alloy nanoparticles with tunable size and surface plasmon resonance frequency, *Chem Mater* 2011, 23:4098
- Treguer M, Cointet C D, Remita H, Khatouri J, Mostafavi M, Amblard J, Belloni J, Dose rate effects on radiolytic synthesis of gold-silver bimetallic clusters in solution, *J Phys Chem B* 1998, 102:4310
- Wang C, Peng S, Chan R, Sun S, Synthesis of AuAg alloy nanoparticles from core/shell-structured Ag/Au, *Small* 2009, 5:567
- Zhang G, Du M, Li Q, Li X, Huang J, Jiang X, Sun D, Green synthesis of Au-Ag alloy nanoparticles using *cucumis sativus* extract, *RSC Adv* 2013, 3:1878
- Liu X, Wang A, Yang X, Zhang T, Mou C Y, Su D S, Li J, Synthesis of thermally stable and highly active bimetallic Au-Ag nanoparticles on inert supports, *Chem Mater* 2009, 21:410
- Petri M V, Ando R A, Camargo P H C, Tailoring the structure, composition, optical properties and catalytic activity of Ag-Au nanoparticles by the galvanic replacement reaction, *Chem Phys Lett* 2012, 531:188
- Wang AQ, Liu JH, Lin SD, Lin TS, Mou CY, A novel efficient Au-Ag alloy catalyst system: preparation, activity, and characterization, *J Catal* 2005, 233:186
- Wang A Q, Chang C M, Mou C Y, Evolution of catalytic activity of Au-Ag bimetallic nanoparticles on mesoporous support for CO oxidation, *J Phys Chem B* 2005, 109:18860
- Kuladeep R, Jyothi L, Alek K S, Deepak K L N, Rao D N, Laser-assisted synthesis of Au-Ag alloy nanoparticles with tunable surface plasmon resonance frequency, *Opt Mater Express* 2012, 2:161
- Kim K, Kim K L, Lee S J, Surface enrichment of Ag atoms in Au/Ag alloy nanoparticles revealed by surface enhanced Raman scattering spectroscopy, *Chem Phys Lett* 2005, 403:77
- Kim K, Kim K L, Choi J Y, Lee H B, Shin K S, Surface enrichment of Ag atoms in Au/Ag Alloy nanoparticles revealed by surface-enhanced Raman scattering of 2,6-dimethylphenyl isocyanide, *J Phys Chem C* 2010, 114:3448
- Fan M, Lai F J, Chou H L, Lu W T, Hwang B J, Brolo A G, Surface-enhanced Raman scattering (SERS) from Au/Ag bimetallic nanoparticles: the effect of the molecular probe, *Chem Sci* 2013, 4:509
- Wang C, Xu L, Xu X, Cheng H, Sun H, Lin Q, Zhang C, Near infrared Ag/Au alloy nanoclusters: tunable photoluminescence and cellular imaging, *J Colloid Interf Sci* 2014, 416:274
- Pal U, Ramírez J F S, Ramírez L N, Álvarez J M, Rojas J A P, Synthesis and optical properties of Au-Ag alloy nanoclusters with controlled composition, *J Nanomater* 2008, 2008:1
- Tong L, Cobley C M, Chen J, Xia Y, Cheng J X, Bright three-photon luminescence from gold/silver alloyed nanostructures for bioimaging with negligible photothermal toxicity, *Angew Chem Int Ed* 2010, 49:3485

16. Jang H, Min D H, Spherically-clustered porous Au-Ag Alloy nanoparticle prepared by partialinhibition of galvanic replacement and its application for efficient multimodal therapy, *ACS Nano* 2015, 9:2696
17. Harun N A, Horrocks B R, Fulton D A, Enhanced Raman and luminescence spectra from co-encapsulated silicon quantum dots and Au–Ag nanoalloys, *Chem Commun* 2014, 50:12389
18. Liu J H, Wang A Q, Chi Y S, Lin H P, Mou C Y, Synergistic effect in an Au-Ag Alloy nanocatalyst: CO oxidation, *J Phys Chem B* 2005, 109:40
19. Xu W, Niu J, Shang H, Shen H, Ma L, Li L S, Facile synthesis of AgAu alloy and core/shell nanocrystals by using Ag nanocrystals as seeds, *Gold Bull* 2013, 46:19
20. Chen H C, Chou S W, Tseng W H, Chen I W P, Liu C C, Liu C, Liu C L, Chen C H, Wu C I, Chou P T, Large AuAg alloy nanoparticles synthesized in organic media using a one-pot reaction: their applications for high-performance bulk heterojunction solar cells, *Adv Funct Mater* 2012, 22:3975
21. Crespo J, Falqui A, Barrasa J G, López-de-Luzuriaga J M, Monge M, Olmos M E, Castillo M R, Sestu M, Soulantica K, Synthesis and plasmonic properties of monodisperse Au–Ag alloy nanoparticles of different compositions from a single-source organometallic precursor, *J Mater Chem C*, 2014, 2:2975
22. Crespo J, Ibarra A, López-de-Luzuriaga M, Monge M, Olmos M E, Synthesis and plasmonic properties of core–shell bimetallic silver–gold nanoprisms obtained through an organometallic route, *Eur J Inorg Chem* 2014, 2014:2383
23. Zhang Q, Xie J, Lee J Y, Zhang J, Boothroyd C, Synthesis of Ag@AgAu metal core/alloy shell bimetallic nanoparticles with tunable shell compositions by a galvanic replacement reaction, *Small* 2008, 4:1067
24. Lu X, Tuan H Y, Chen J, Li Z Y, Korgel B A, Xia Y, Mechanistic studies on the galvanic replacement reaction between multiply twinned particles of Ag and HAuCl<sub>4</sub> in an organic medium, *J Am Chem Soc* 2007, 129:1733
25. Ferrer D A, Torres L A D, Wu S, Yacaman M J, Crystalline order of silver–gold nanocatalysts with hollow-core and alloyed-shell, *Catal Today* 2009, 147:211
26. Choi Y, Hong S, Liu L, Kim S K, Park S, Galvanically replaced hollow Au–Ag nanospheres: study of their surface plasmon resonance, *Langmuir* 2012, 28:6670
27. Sun Y, Xia Y, Alloying and dealloying processes involved in the preparation of metalnanoshells through a galvanic replacement reaction, *Nano Lett* 2003, 3:1569
28. Sun Y, Xia Y, Multiple-walled nanotubes made of metals, *Adv Mater* 2004, 16:264
29. Sun Y, Silver nanowires-unique templates for functional nanostructures, *Nanoscale* 2010, 2:1626
30. Sun Y, Xia Y, Mechanistic study on the replacement reaction between silver nanostructures and chloroauric acid in aqueous medium, *J Am Chem Soc* 2004, 126:3892
31. Tung H T, Chen I G, Song J M, Yen C W, Thermally assisted photoreduction of vertical silver nanowires, *J Mater Chem* 2009, 19:2386
32. Chen H N, Liu R S, Jang L Y, Lee J F, Hu S F, Characterization of core–shell type and alloy Ag/Au bimetallic clusters by using extended X-ray absorption fine structure spectroscopy, *Chem Phys Lett* 2006, 421:118
33. Tao A, Kim F, Hess C, Goldberger J, He R, Sun Y, Xia Y, Yang P, Langmuir-blodgett silver nanowire monolayers for molecular sensing using surface-enhanced Raman spectroscopy, *Nano Lett* 2003, 3:1229
34. Link S, Wang Z L, El-Sayed M A, Alloy formation of gold-silver nanoparticles and the dependence of the plasmon absorption on their composition, *J Phys Chem B* 1999, 103:3529
35. Johnson R C, Li J, Hupp J T, Schatz G C, Hyper-rayleigh scattering studies of silver, copper and platinum nanoparticle suspensions, *Chem Phys Lett* 2002, 356:534
36. Slater, T J A, Macedo A, Schroeder S L M, Burke M G, O'Brien P, Camargo P H C, Haign S J, Correlating catalytic activity of Ag–Au nanoparticles with 3D compositional variations, *Nano Lett* 2014, 14:1921.
37. Sun Y G, Mayers B T, Xia Y N, Template-engaged replacement reaction: A one-step approach to the large-scale synthesis of metal nanostructures with hollow interiors, *Nano Lett* 2002, 2:481
38. Sun Y, Xia Y, Shape-controlled synthesis of gold and silver nanoparticles, *Science* 2002, 298:2176
39. Yin Y, Erdonmez C, Aloni S, Alivisatos A. Paul, Faceting of nanocrystals during chemical transformation: from solid silver spheres to hollow gold octahedra, *J Am Chem Soc* 2006, 128:12671
40. Massalski TB, Okamoto H, Subramanian PR, Kacprzak L (1990) Binary alloy phase diagrams, 2nd edn. ASM International, Materials Park, OH

**Submit your manuscript to a SpringerOpen® journal and benefit from:**

- Convenient online submission
- Rigorous peer review
- Immediate publication on acceptance
- Open access: articles freely available online
- High visibility within the field
- Retaining the copyright to your article

Submit your next manuscript at ► [springeropen.com](http://springeropen.com)